Twelfth Australasian Fluid Mechanics Conference
The University of Sydney, Australia 1995

A NUMERICAL STUDY OF BUBBLE MOTION IN A GRAVITATIONAL FIELD

L. Chen, J.A. Reizes and E. Leonardi
School of Mechanical and Manufacturing Engineering,
The University of New South Wales
Sydney, 2052
Australia

ABSTRACT

One of the difficulties in numerical modelling two phase flow is the tracking of the interface between the phases. This is also true for large gas bubbles moving under the action of gravity in a liquid filled enclosure. Numerical models for two and three-dimensional bubble motion are presented using a modified VOF method which takes into account the effects of surface tension. Examples are presented to illustrate the effects of density, viscosity and surface tension variations on bubble motion in an axisymmetric situation. An example of three-dimensional solution is also presented.

INTRODUCTION

Recent progress in the understanding of complex single-phase flows can be attributed to the development of fluid visualisation techniques, detailed velocity measurements and the increasing power of numerical simulation. However, difficulties are still encountered, experimentally and numerically, in flows which consist of two or more phases. In numerical work the difficulties are associated with accurately determining the motion of the interface delineating a gas bubble in a liquid. The main problem is the numerical diffusion of the advancing interface which destroys the sharpness of the front. A few higher order numerical schemes can reduced this artificial diffusion but may cause oscillations (Unverdi and Tryggvason 1992).

In order to fully understand the behaviour of a multi-fluid system, a good insight is required into the basic micromechanisms of a single structure. Volume tracking methods can simply and accurately account for the interaction of many different smoothly varying interfaces. The VOF method, introduced by Hirt and Nichols (1981), is a variation of the MAC method. Here, the massless particles used in the MAC method are replaced by a function, F, which represents the fractional volume of a cell occupied by the liquid phase. F is convected by the velocity field so that an equation can be written for its transport. The orientation and location of the interface is then determined by the value of F in the interface cells - that is in the region where F changes from zero to one.

MATHEMATICAL FORMULATION

Here, the motion of a gas bubble in an otherwise stationary liquid is studied using a modified VOF method which incorporates surface tension stresses. Since the pressure changes are very small, the equations of motion for both fluids are given by the incompressible Navier-Stokes and continuity equations which in conservative form are

$$\frac{\partial(\rho\mathbf{U})}{\partial t} + \nabla \bullet (\rho\mathbf{U} \otimes \mathbf{U}) = -\nabla p + \nabla \times (\mu \nabla \times \mathbf{U}) + \rho\mathbf{g} + \mathbf{F}_{sv} \qquad (1)$$

and

$$\nabla \bullet \mathbf{U} = \frac{1}{\rho}\frac{D\rho}{Dt}, \qquad (2)$$

in which, $\mathbf{U}(\mathbf{x},t) = (u_r, u_\theta, u_z)$ is the fluid velocity, $\mathbf{x}(r,\theta,z)$ is the position, ρ is the density, μ is the dynamic viscosity, p is the pressure, $\mathbf{g}$ is the gravitational acceleration vector and $\mathbf{F}_{SV}$ is the volume form of the surface tension force and which appears only at the interface. The right hand side of equation (2) is equal to zero if both liquid and gas densities are constant. It should be noted that both ρ and μ have different values for the liquid and gas phases and at the interface. This discontinuity can be used to represent the interface.

However, the ratio of the density and dynamic viscosity for water and air is of the order of 850 and this sharp discontinuity makes numerical simulation very difficult. Instead of solving equation (2) directly, the function F, which lies between 0 and 1, and as mentioned above is

used as a indicator of the interface, is evaluated following Hirt and Nichols (1981) from,

$$\frac{\partial F}{\partial t} + \nabla \bullet (\mathbf{U}F) = 0 \qquad (3)$$

At the interface, the density and viscosity to be used in equations (1 and 2) can be expressed as

$$\rho(\mathbf{x},t) = F(\mathbf{x},t)\rho_f + [1 - F(\mathbf{x},t)]\rho_g \qquad (4)$$

$$\mu(\mathbf{x},t) = F(\mathbf{x},t)\mu_f + [1 - F(\mathbf{x},t)]\mu_g \qquad (5)$$

Following Brackbill *et al* (1992), $\mathbf{F_{SV}}$ can be written as

$$\mathbf{F}_{sv}(\mathbf{x},t) = \sigma\kappa(\mathbf{x},t)\mathbf{n} \qquad (6)$$

where σ is the coefficient of surface tension and κ is the curvature of the interface. κ may be calculated from:

$$\kappa(\mathbf{x},t) = \frac{1}{|\mathbf{n}|}\left[\left(\frac{\mathbf{n}}{|\mathbf{n}|} \bullet \nabla\right)|\mathbf{n}| - (\nabla \bullet \mathbf{n})\right] \qquad (7)$$

in which,

$$\mathbf{n} = \nabla F \qquad (8)$$

The computational domain has been divided into a number of non overlapping control volumes so that one control volume surrounds each grid point and all variables are defined at the centre of the control volume. The differential equations are integrated over each control volume. In the fully implicit scheme, a forward step in time is used, so that the equation is written for any variable ϕ as

$$\frac{\phi^{n+1} - \phi^n}{\Delta t} = f(\phi^{n+1}) + s \qquad (9)$$

in which the superscript n indicates the nth time step and s is the source term. The discretized equations obtained in such a manner more accurately represent the conservation of mass and momentum than the more familiar finite difference approximations and have therefore been used here. For a finite control volume centred at the point *P(i,j,k)* equations (9) can be written as

$$A_P\phi_P = \sum A_{NP}\phi_{NP} + s_P \qquad (10)$$

in which A is the coefficient which results from the discretization and the subscripts P and N denote the centre point of a control volume and the neighbouring volumes surrounding P respectively.

Since oscillations in pressure and velocity fields may result when a non-staggered grid is used, the Rhie and Chow (1982) interpolation has been employed. For example the solution of equation (10) with $\phi = u_r$ becomes,

$$u_{r,P} = \frac{\sum A_{NP}u_{r,NP} + S_P}{A_P} + B_P\nabla p_P = \hat{u}_{r,P} + B_P\nabla p_P \qquad (11)$$

in which B is the coefficient of the pressure gradient term. The velocity on the right face of a control volume centred on P(i,j,k) is given by

$$u_{r,e,i,j,k} = \frac{(\hat{u}_{r,i,j,k} + \hat{u}_{r,i+1,j,k})}{2} + \frac{(B_{i,j,k} + B_{i+1,j,k})}{2}\nabla p_{e,i,j,k} \qquad (12)$$

The pressure-velocity coupling is based on the SIMPLE algorithm introduced by Patankar (1983). If the velocity and pressure are defined as

$$\begin{aligned} \mathbf{U} &= \mathbf{U}^* + \mathbf{U}' = \mathbf{U}^* + B\nabla p' \\ p &= p^* + p' \end{aligned} \qquad (13)$$

in which, p' and $\mathbf{U}'$ are the pressure and velocity corrections respectively, p^* is the value of the pressure at the previous step and $\mathbf{U}^*$ is the solution obtained from equation (10). The pressure correction is obtained by substituting equation (13) into equation (2), yielding in general

$$\nabla \bullet (B\nabla p') = \nabla \bullet \mathbf{U}^* \qquad (14)$$

At each time step, values of p obtained from equations (14) and (13) are used in equation (11) and new values of $\mathbf{U}^*$ obtained. The pressure is updated by solving equation (14). The iterations are continued until $\nabla \bullet \mathbf{U}^* \approx 0$. Once this has been achieved, equation (11) is progressed to the next time step. Equation (4) is solved by a modified DONOR-ACCEPTOR cell algorithm. A correction is performed on the basis of the residual resulting from the continuity equation.

We now require suitable boundary conditions. In the cases discussed in this paper the initially spherical gas bubble is located on the axis of a vertical closed cylinder otherwise filled with a stationary liquid. The boundary conditions on the walls are $\mathbf{U} = \nabla p' = 0$. The bubble is initially at rest and is a perfect sphere.

The axisymmetric solutions have been obtained on a two-dimensional (r,z) grid with all θ derivatives set to zero. Although not discussed here a mesh refinement study indicated that a 34x80 mesh leads to sufficiently accurate solutions for the axisymmetric case, so that this mesh has been used in this study. A 12x8x40 mesh was used in the three dimensional case.

RESULTS AND DISCUSSION

In non-dimensional form, the bubble deformation and its motion can be characterised by the Morton number $M = g\mu_f^4 / \rho_f\sigma^3$, the Bond number $Bo = \rho_f g d_e^2 / \sigma$, the density ratio ρ_f/ρ_g, viscosity ratio μ_f/μ_g and the initial cylinder to bubble radius ratio (R_c/R_b). We have performed a parametric study of an asymmetric bubble with $5\text{x}10^{-6} \le M \le 50$, $42 \le Bo \le \infty$, $10 \le \rho_f/\rho_g \le 1000$, $40 \le \mu_f/\mu_g \le 100$ and $1.5 \le R_c/R_b \le 2.5$. Due to the restriction on the length of this paper, only a very small sample of results is presented here.

The results for M=7.4x10^{-2}, Bo=420, ρ_f/ρ_g=1000 and μ_f/μ_g=80 and R_c/R_b=2.0 are shown in Figure 1. As the bubble begins to rise due to buoyancy (Figure 1(a)), a jet forms at the bottom of the bubble and pushes the lower surface upwards (Figure 1(b)). The velocity of the upper surface of the bubble decreases with increasing time, so that the bubble becomes a shell (Figures 1(c)).

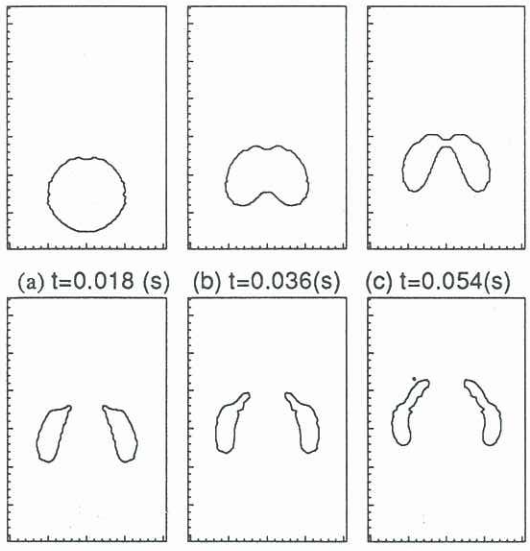

FIGURE 1 BUBBLE MOTION IN A CYLINDER
($M=7.4\times10^{-2}$, $Bo=420$, $\rho_f/\rho_g=1000$, $\mu_f/\mu_g=80$, $R_c/R_b=2.0$)

As time progresses the lower surface approaches the top surface and eventually pierces it, thus forming a toroid (Figure 1(d)). At a later time still, the toroid expands as may be seen by comparing Figures 1 (e) and (f). Walters and Davidson (1963) experimentally observed similar phenomena.

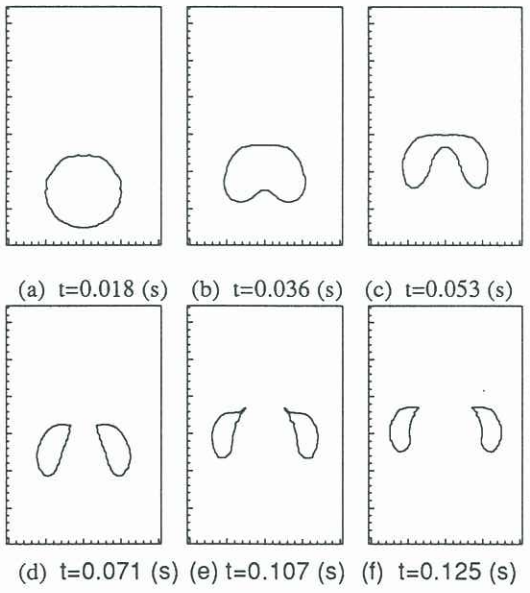

FIGURE 2 A BUBBLE MOTION IN A CYLINDER
($M=7.8\times10^{-5}$, $Bo=50$, $\rho_f/\rho_g=100$, $\mu_f/\mu_g=80$, $R_c/R_b=2.0$)

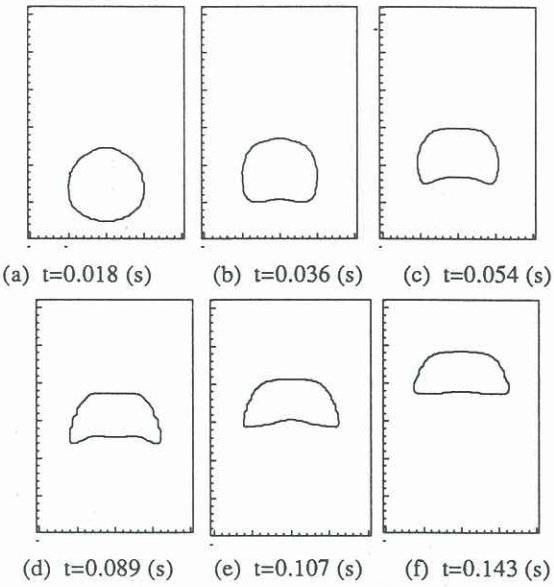

FIGURE 3 A BUBBLE MOTION IN A CYLINDER
($M=1.25\times10^{-2}$, $Bo=5$, $\rho_f/\rho_g=40$, $\mu_f/\mu_g=40$, $R_c/R_b=2.0$)

If the values of *Bo*, the density ratio and *M* are changed to 50, 100 and 7.8×10^{-5} respectively, the flows show in Figure 2 result. It may be seen that a decrease in Bond number and density ratio leads to a slightly different sequence of shapes to those shown in Figure 1 and the diameter of the toroid decreases due to the smaller density ratio and higher surface tension. A lower viscosity does not significantly affect the initial shape of the bubble, but a shorter toroid finally evolves (see Figure 2).

In Figure 3 it can seen that an increase in the coefficient of surface tension together with a further reduction in the density and viscosity ratios leads to an inverted cup shape. Although initially a weak water jet is formed (Figures 3(b) and (c)) it does not pierce the bubble.

An example of a three-dimensional solution is presented in Figure 4. The shape development is the similar to that in Figures 1 and 2. It should be noted that the views in Figure 4 have been chosen so as to yield a good understanding of the shape development of the bubble.

The bubble position history is shown in Figure 5. It can be seen that the velocity changes depending on the parameters used. When $Bo \geq 50$, the bubble breaks into a toroid. Under those circumstance, a higher density ratio leads to a more quickly rising bubble. A bigger surface tension force , ie. small value of *Bo*, causes a slow bubble translation. A high surface tension leads to an inverted cup bubble, which travels faster than a toroid even for a low density ratios.

The current method has been extended to include mass and heat transfer and their effects are now being studied.

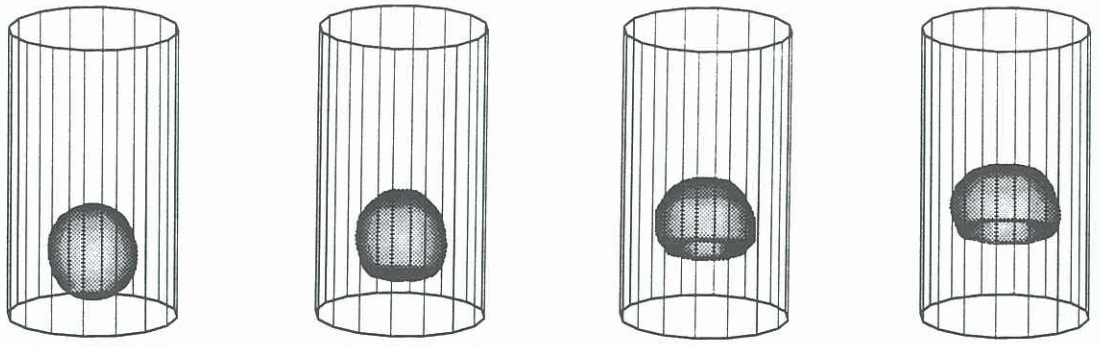

(a) t=0.004 (s) (b) t=0.021 (s) (c) t=0.039 (s) (d) t=0.057 (s)

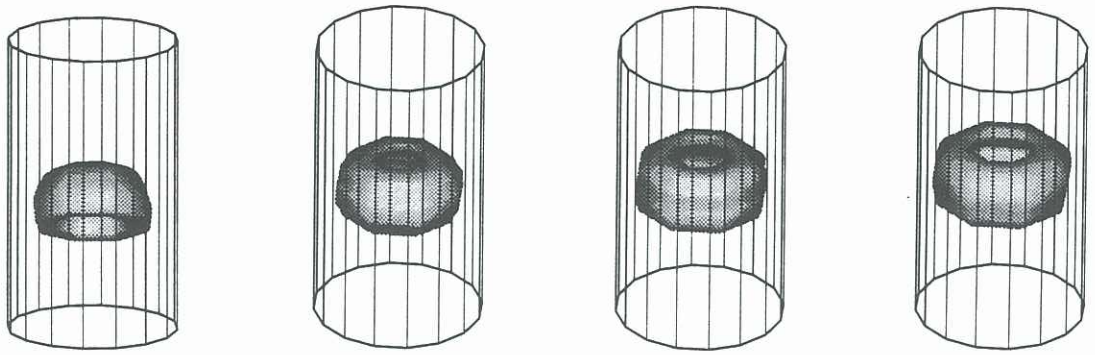

(e) t=0.075 (s) (f) t=0.093 (s) (g) t=0.12 (s) (h) t=0.13 (s)

FIGURE 4 A BUBBLE MOTION IN THREE DIMENSIONAL
($M=5.0X10^{-6}$, Bo=420, $\rho_f / \rho_g = 80$, $\mu_f / \mu_g = 80$, $R_c/R_b=2.0$)

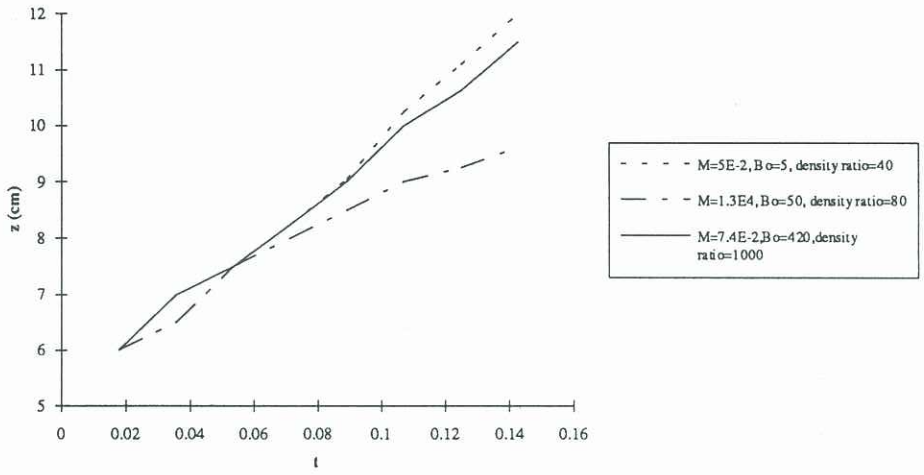

FIGURE 5 THE EFFECT OF VISCOSITY AND SURFACE TENSION ON BUBBLE MOTION

REFERENCE

Brackbill, J.U., Kothe, D.B. and Zemach, C., (1992), "A Continuum Method for Modeling Surface Tension", *J. Comput. Phys* Vol. 100, pp. 335-354.

Hirt, C.W. and Nichols, B.D., (1981), "Volume of Fluid (VOF) Method for the Dynamics of Free Boundary", *J. Comput. Phys* Vol. 39, pp. 201-225.

Patankar, S.V. (1983), "Numerical Heat Transfer and Fluid Flow", Washington DC ,Hemisphere.

Rhie, C.M. and Chow. W.L., (1982), "Numerical Study of Turbulent Flow Past an Airfoil with Trailing Edge Separation", *AIAA, J1* Vol. 21 pp. 1527-1532.

Unverdi, S.O., Tryggvason, G., (1992), "Computations of Multi-Fluid Flows", *Physica D,* Vol. 60, pp. 70-83.

Walters, J.K and Davidson, J.F., (1963), "The Initial Motion of a Gas Bubble Formed in an Inviscid Liquid", *J. Fluid Mech.* Vol. 17, pp. 321-336.